

Diethyl Oxaloacetate. Nonconcerted General Catalysis of Enolization, Tertiary Amine Catalyzed Enolization via an Addition–Elimination Mechanism, and General-Acid-Catalyzed Dehydration and Cleavage

Paula Yurkanis Bruice and Thomas C. Bruice*

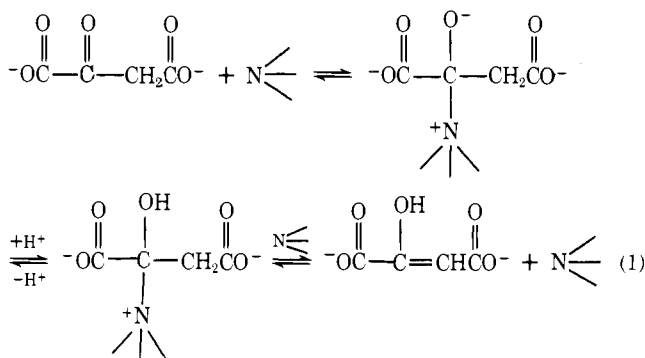
Contribution from the College of Creative Studies and the Department of Chemistry, University of California at Santa Barbara, Santa Barbara, California 93106.

Received October 28, 1976.

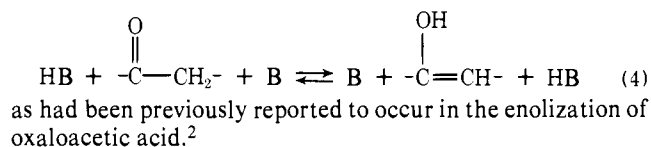
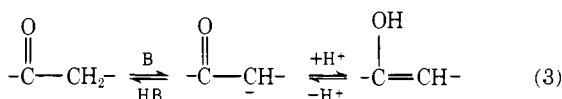
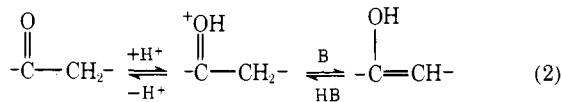
Abstract: In the presence of lyate species, diethyl oxaloacetate evidences rate processes for establishment of both ketonization–enolization and hydration–dehydration equilibria. Both reactions show acid, spontaneous, and base catalyzed pathways. No evidence was obtained for the occurrence of concerted general acid–general base catalysis of the enolization reaction; only stepwise catalysis is observed. The dehydration reaction is catalyzed by general acids; the second-order general acid catalytic rate constants give a $-\alpha$ value of 0.62. Tertiary amines of $pK_a > 8$ catalyze the enolization reaction via the formation of a zwitterionic carbinolamine intermediate followed by amine-catalyzed elimination of a proton + amine from protonated carbinolamine. Elimination apparently occurs only through the protonated intermediate. A β of 0.45 is obtained from the second-order rate constants for attack of tertiary amines on diethyl oxaloacetate, indicating less sensitivity to amine pK_a than was found for the reaction of tertiary amines with the less reactive diacid ($\beta = 0.77$). After enolization is complete, tertiary amines act as general acids ($-\alpha = 0.89$) to catalyze a reaction that is suggested to be cleavage of the zwitterionic carbinolamine to oxalate and acetate. The pK_a of enolic diethyl oxaloacetate was determined by titration to be 8.0, while the kinetically apparent pK_a of the ketone carbon acid was found to be 10.05.

Introduction

In an investigation of the enolization of oxaloacetic acid we found that tertiary amines of $pK_a > 8$ did not catalyze the reaction by the expected general-base-catalyzed mechanism.¹ The mechanism of eq 1, which involves initial carbinolamine



formation followed by an amine-catalyzed E_2 elimination of a proton and neutral amine, was proposed to account for the superior catalytic ability of tertiary amines. Heretofore, carbinolamine formation had been recognized only with primary and secondary amines which were known to catalyze the enolization of ketones via formation of an intermediate imine. Less basic tertiary amines and oxyanion bases such as phosphate and carbonate are apparently not sufficiently nucleophilic to allow formation of an intermediate with oxaloacetic acid, and thus they catalyze the enolization reaction via the stepwise general-acid- and/or general-base-catalyzed mechanisms of eq 2 and 3. No evidence was obtained for the existence of concerted general acid–general base catalysis (eq 4),



Since carbinolamine intermediates had not formerly been noted in tertiary amine catalyzed enolization reactions, we undertook an investigation of the enolization of the diethyl ester of oxaloacetic acid in order to determine whether tertiary amines would also act as nucleophilic catalysts in the enolization of this more reactive ketone. In addition, we were interested in ascertaining whether the general-acid- and general-base-catalyzed keto–enol interconversion of diethyl oxaloacetate occurs solely in a stepwise mechanism as with oxaloacetic acid. The results of this study are reported herein.

Experimental Section

The sodium salt of diethyl oxaloacetate (Eastman, lot no. 43B) was used without further purification. Anal. Calcd for $\text{C}_8\text{H}_{11}\text{O}_5\text{Na}$: C, 45.72; H, 5.28; Na, 10.94. Found: C, 45.85; H, 5.27; Na, 10.84. Ketone formation was monitored employing a stock solution of enolic diester in ethanol. An aqueous (0.5 M KCl, 10^{-4} M EDTA, pH 8.0) stock solution containing a keto–enol equilibrium mixture was employed to monitor the approach to new equilibrium mixtures at varying pHs (Figure 1). The concentrations of the stock solutions were such that upon dilution with buffer or with 0.5 M KCl a kinetic solution was provided which was 1×10^{-4} M in ester. The kinetic determinations were carried out at 30.0 ± 0.2 °C in doubly glass-distilled water with the ionic strength maintained at 0.5 with KCl. All kinetic solutions contained 10^{-4} M EDTA in order to scavenge extraneous metal ions. Rate constants were determined by monitoring the change in absorption at 270 or 250 nm. Because of the rapid rate of the reactions investigated, the majority of the rate determinations were carried out with a Durrum-Gibson Model 13001 stopped-flow spectrophotometer in which case an aqueous solution of the diester (pH 8.0) was mixed with the appropriate buffer solution. Pseudo-first-order conditions of $[\text{buffer}]_T \gg [\text{diethyl oxaloacetate}]$ were employed. In the absence of buffers, rate constants were determined either in a Radiometer pH-stat assembly specifically designed for a Cary 15 spectrophotometer⁵ or with a stopped-flow spectrophotometer in which case a determination was made of the pH of the reaction solution after mixing. All pK_a s were determined by half-neutralization at 30 °C and $\mu = 0.5$ (KCl).

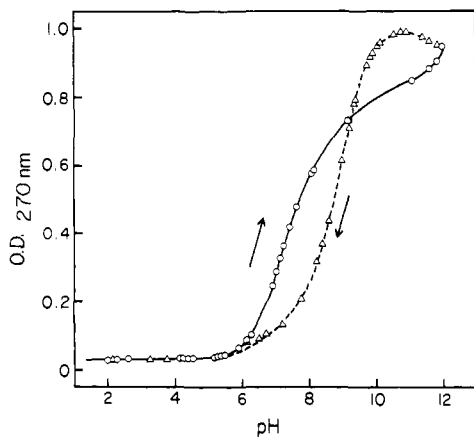


Figure 1. The absorbance at 270 nm of an aqueous solution of diethyl oxaloacetate (2.8×10^{-5} M, 30°C , $\mu = 0.5$) as a function of pH. The solid line refers to titration with base and the dashed line to back-titration with acid. Each absorbance value was read 20 s after addition of an aliquot of acid or base. All points have been corrected for dilution effects.

Purification of buffers, preparation of buffer solutions, and methods of calculation have been described previously.¹

Results and Discussion

Diethyl oxaloacetate exists in aqueous solution as a mixture of keto, enol, and hydrated species. Below pH 6 the absorbance (270 nm) of a 2.8×10^{-5} M solution of the diester is constant (Figure 1). As the pH is increased above 6, the absorbance increases due to the formation of increasing concentrations of enolate anion. From the figure it is apparent that the pK_a of the enol tautomer is approximately 8.0. Increasing the pH above 9.5 indicates the presence of another ionizing species with a pK_a greater than that of the enol. Back-titration of the equilibrium mixture results in a different titration curve, characteristic of a compound in which proton donation is at a site different from that of proton removal. From the pH-rate profile (a) of Figure 2, a kinetically apparent pK_a of 10.05 (see also eq 5) is obtained for the dissociation of a proton from the α -carbon atom of diethyl oxaloacetate. Thus, the unusual titration curve of Figure 1 is explained by the fact that as an acidic solution of the keto-enol equilibrium mixture is made more basic a proton is first lost from the enol oxygen, the more acidic of the two tautomers. When, however, acid is added to a basic solution of the tautomers, the more basic carbon is the first to accept a proton to yield ketone, and nonsuperimposable titration curves result. The pK_a s of 8.0 and 10.05 obtained for the enol and keto tautomers, respectively, of diethyl oxaloacetate are in relative agreement with previously reported pK_a s of keto-enol tautomers.⁶ For example, the enol and keto forms of ethyl acetoacetate have pK_a s of 7.3 and 10.7, respectively.⁷ In the previous study of the enolization of oxaloacetic acid, nonsuperimposable forward and reverse titration curves were not observed, since hydrogen bonding of the enolic proton to the negatively charged carboxylate group increases its pK_a (13.03 determined by 25°C)⁸ to a value close to that of the ketone (kinetically apparent pK_a of 12.75 at 30°C).¹

Lyate Species Catalysis. Diethyl oxaloacetate, at any constant pH and in the absence of buffer, undergoes two consecutive pseudo-first-order reactions which lead to the two pH-rate profiles indicated by the solid lines in Figure 2. The observed rate constants indicated by circles on profile 2a were obtained using an equilibrated aqueous stock solution of diethyl oxaloacetate at pH 8. As predicted by Figure 1, the observed rate constants below pH 8 pertain to a reaction that evidences decreasing absorption with time (indicative of overall ketonization), while those above pH 8 show increasing absorption (enolization). Rate constants (triangles) on profile 2a were also

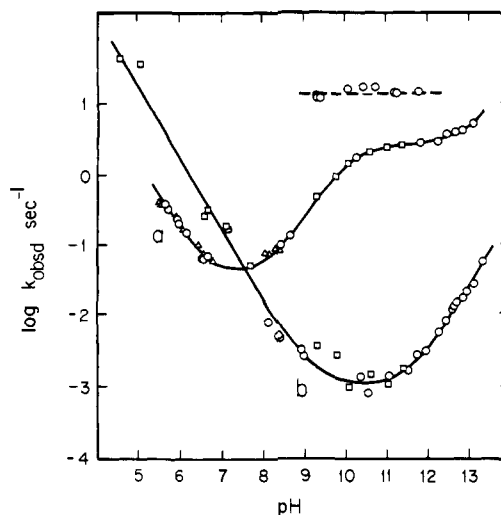


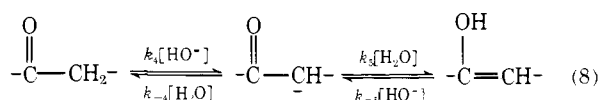
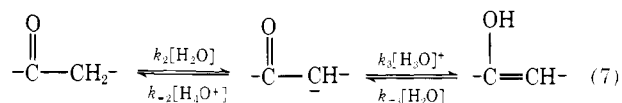
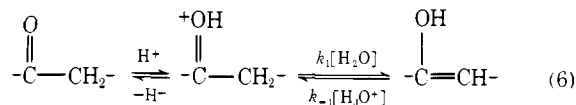
Figure 2. Line a: pH-rate profile for keto-enol interconversion of diethyl oxaloacetate (H_2O , 30°C , $\mu = 0.5$). Rates determined solely in the presence of lyate species (an autotitration assembly was used below pH 9) employing primarily the keto tautomer as substrate (O) and the enol tautomer as substrate (Δ), and rates determined from intercepts of carbonate and phosphate ($\text{HPO}_4^{-2}/\text{PO}_4^{-3}$) buffer dilution plots (\square). Line b: pH-rate profile for establishment of the hydration-dehydration equilibrium of diethyl oxaloacetate (H_2O , 30°C , $\mu = 0.5$). Rates determined with an autotitrator assembly (O) and rates determined from intercepts of buffer dilution plots employing acetate, imidazole, phosphate ($\text{H}_2\text{PO}_4^-/\text{HPO}_4^{-2}$ and $\text{HPO}_4^{-2}/\text{PO}_4^{-3}$), and carbonate buffers (\square). Dashed line: Intercepts obtained by extrapolation of the linear portions of amine buffer dilution plots at high $[\text{N}]_T$ to $[\text{N}]_T = 0$. All points are experimental and the theoretical lines were generated from eq 5 and 13.

determined using a stock ethanolic solution of enolic diethyl oxaloacetate and measuring the rate of decrease in absorption. The line connecting the experimental points of the pH-rate profile of Figure 2a was computer generated from the following empirical equation

$$k_{\text{obsd}} = k_{\text{H}}a_{\text{H}} + k_{\text{c}} + k_{\text{b}} \left(\frac{K_{\text{a}}}{K_{\text{a}} + a_{\text{H}}} \right) + k_{\text{HO}^-} \frac{K_{\text{w}}}{a_{\text{H}}} \quad (5)$$

where $k_{\text{H}} = 1.5 \times 10^5 \text{ M}^{-1} \text{ s}^{-1}$, $k_{\text{c}} = 3.4 \times 10^{-2} \text{ s}^{-1}$, $k_{\text{b}} = 2.5 \text{ s}^{-1}$, $k_{\text{HO}^-} = 15 \text{ M}^{-1} \text{ s}^{-1}$, $pK_{\text{a}} = 10.05$, $pK_{\text{w}} = 13.83$, and a_{H} is the hydrogen-ion concentration as determined at the glass electrode.

The pH-rate profile of Figure 2a is attributed to keto-enol interconversion of diethyl oxaloacetate according to the acid-, water-, and base-catalyzed mechanisms of eq 6-8. In aqueous solution at constant pH, proton transfer to and from oxygen may be assumed to be rapid and to be controlled by the pH and the pK_a of protonated ketone and neutral enol; thus, the rate-limiting steps of eq 6-8 may be assumed to be proton removal from carbon in the forward direction and proton donation to carbon in the reverse direction. Since the pH-dependent rate constant for approach to equilibrium (k_{obsd}) is given by the sum of the forward (k_{f}) and reverse (k_{r}) rate constants, the kinetic expressions for the mechanisms of eq 6-8, assuming equilib-



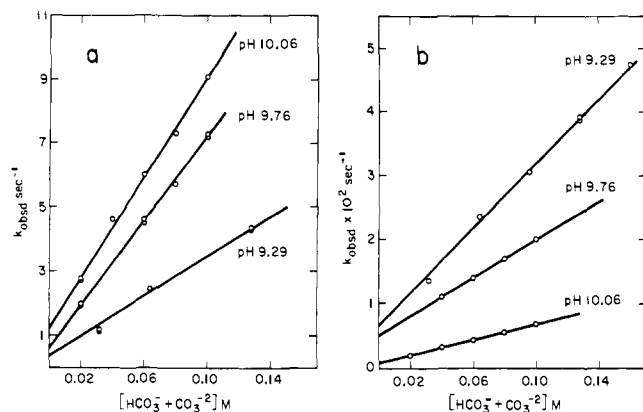


Figure 3. (a) Plots of the observed first-order rate constants for the initial reaction of diethyl oxaloacetate in the presence of carbonate buffer vs. the total concentration of carbonate buffer at three hydrogen ion concentrations. (b) Plots of the observed first-order rate constants for the second reaction evidenced by diethyl oxaloacetate in the presence of carbonate buffer.

rium between ketone and protonated ketone and enol and enolate anion, are given by eq 9–11, respectively, where K_E , K_K , and K_{CH} are the acid-dissociation constants of enol, protonated ketone, and ketone carbon acid. Summation of eq 9–11 leads

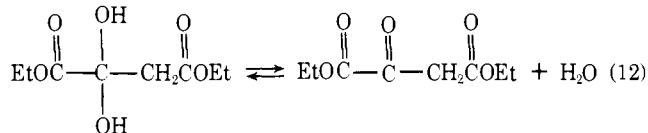
$$k_{\text{obsd}} = k_f + k_r = k_1[\text{H}_2\text{O}] \frac{a_{\text{H}}}{K_K + a_{\text{H}}} + k_{-1}a_{\text{H}} \left(\frac{a_{\text{H}}}{K_E + a_{\text{H}}} \right) \\ = \left(\frac{k_1[\text{H}_2\text{O}]}{K_K} + k_{-1} \right) a_{\text{H}}, \text{ since } K_K > a_{\text{H}} \text{ and } a_{\text{H}} > K_E \quad (9)$$

$$k_{\text{obsd}} = k_f + k_r = k_2[\text{H}_2\text{O}] + k_{-2}a_{\text{H}} \left(\frac{K_{\text{CH}}}{K_{\text{CH}} + a_{\text{H}}} \right) \\ = k_2[\text{H}_2\text{O}] + k_{-2}K_{\text{CH}}, \text{ since } a_{\text{H}} > K_{\text{CH}} \quad (10)$$

$$k_{\text{obsd}} = k_f + k_r = k_4[\text{HO}^-] + k_{-4}[\text{H}_2\text{O}] \left(\frac{K_{\text{CH}}}{K_{\text{CH}} + a_{\text{H}}} \right) \quad (11)$$

to the general kinetic expression of eq 5. Thus, the k_b term of eq 5 refers to the rate of protonation ($k_{-4}[\text{H}_2\text{O}]$) of the α -carbon atom and, as expected, is slower for diethyl oxaloacetate (2.5 s^{-1}) than for oxaloacetic acid (38 s^{-1});¹ the K_a term of eq 5 is the dissociation constant of the ketone carbon acid ($\text{p}K_{\text{app}} = 10.05$ for diethyl oxaloacetate vs. 12.75 for oxaloacetic acid);¹ and k_{HO^-} is the second-order rate constant for proton removal from the α -carbon atom (k_4), which occurs more readily from diethyl oxaloacetate ($15 \text{ M}^{-1} \text{ s}^{-1}$) with its electron-withdrawing $-\text{COOEt}$ groups than from oxaloacetate ($5 \text{ M}^{-1} \text{ s}^{-1}$) with carboxylate anion groups. The water-catalyzed reaction of eq 7 is not evidenced by the less-reactive diacid.

The second pH-rate profile, b of Figure 2, may be ascribed to establishment of the hydration–dehydration equilibrium of eq 12. Because this is a reversible process, the observed rate



constants plotted on line b of Figure 2 refer to a sum of rate constants ($k_{\text{hydration}} + k_{\text{dehydration}}$). The reaction in the absence of buffer species above pH 8 evidences increasing absorption with time, indicating that the overall reaction, initiated by addition of the substrate equilibrium mixture at pH ~ 8 to a more basic solution, is in the direction of dehydration. The hydration equilibrium does not necessarily change above pH 8. However, since conversion of ketone to enolate anion increases with increasing pH, the concentration of hydrate must

decrease to reestablish the keto–hydrate equilibrium. The line drawn through the experimental points was computer generated from the empirical eq 13,

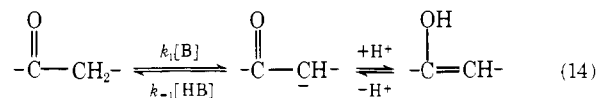
$$k_{\text{obsd}} = k_{\text{HAH}} + k_0 + k_{\text{HO}^-} \left(\frac{K_{\text{w}}}{a_{\text{H}}} \right) \quad (13)$$

where $k_{\text{H}} = 1.7 \times 10^6 \text{ M}^{-1} \text{ s}^{-1}$, $k_0 = 1 \times 10^{-3} \text{ s}^{-1}$, and $k_{\text{HO}^-} = 1.7 \times 10^{-1} \text{ M}^{-1} \text{ s}^{-1}$. Acid-catalyzed, spontaneous, or water-catalyzed, and base-catalyzed pathways for approach to hydration equilibrium have previously been reported for a variety of carbonyl compounds. Rate constants for the uncatalyzed reaction range from 1×10^{-4} to $3 \times 10^{-2} \text{ s}^{-1}$ at 25°C .⁹

A hydration–dehydration equilibrium was not observed with oxaloacetic acid above about pH 5. It has been reported that oxaloacetic acid exists as the hydrate in aqueous solution at pH 6.89 to an extent of only 5.2%.¹⁰ It is not surprising that the oxaloacetic acid dianion has considerably less tendency to hydrate than does the diester, since the electron-withdrawing $-\text{COOEt}$ ($\sigma_{\text{I}} = 0.34$) and $-\text{CH}_2\text{COOEt}$ ($\sigma_{\text{I}} = 0.13$) groups have been replaced by an electron-donating $-\text{COO}^-$ ($\sigma_{\text{I}} = -0.17$) group and a weakly electron-withdrawing $-\text{CH}_2\text{COO}^-$ ($\sigma_{\text{I}} = 0.01$) group.¹¹

Two additional rate processes, which are not shown in Figure 2, are observed in the presence of lyate species after the hydration–dehydration equilibrium of eq 12 has been established. The first of these exhibits a pH-independent region from pH 7 to 10 ($k_{\text{obsd}} = 1.7 \times 10^{-4} \text{ s}^{-1}$) and gives evidence of hydroxide ion dependence in more basic solutions. This reaction may likely be ascribed to ester hydrolysis. The second process is extremely slow ($k_{\text{obsd}} < 10^{-5} \text{ s}^{-1}$) and may be due to hydrolysis of the second ester group or to decarboxylation.

Buffer Catalysis. The reaction of diethyl oxaloacetate in the presence of carbonate buffer ($\text{p}K_a$ 9.76) gives rise to linear buffer dilution plots (Figure 3a), and the pH dependence of the slopes of the plots indicates dependence of rate on $[\text{CO}_3^{2-}]$. Linear buffer dilution plots were also obtained with phosphate buffer ($\text{HPO}_4^{2-}/\text{PO}_4^{3-}$, $\text{p}K_a$ 11.36). The pH dependence of the slopes of these plots, however, indicates that the rate increases with increasing concentration of the acid component of the buffer (Figure 4a). The intercepts of the carbonate and phosphate buffer dilution plots at zero buffer concentration are indicated by the squares on pH–rate profile a of Figure 2 at pHs > 9 . Thus, these buffer dilution plots pertain to what we have ascribed to a base-catalyzed keto–enol interconversion (eq 8). The linearity of the buffer dilution plots requires that proton removal and proton donation occur sequentially (eq 14).



No evidence was obtained for the operation of the concerted general acid–general base catalyzed mechanism of eq 4 with any of the buffers employed in this study. The observed rate constants plotted in Figures 3a and 4a may be described by the rate law of eq 15 where k_{1y} is the contribution to catalysis in

$$k_{\text{obsd}} = k_f + k_r = k_1[\text{B}] + k_{-1} \left(\frac{K_{\text{CH}}}{K_{\text{CH}} + a_{\text{H}}} \right) [\text{HB}] + k_{1y} \quad (15)$$

the forward and reverse direction by lyate species. In the case of carbonate buffer solutions, $a_{\text{H}} \geq K_{\text{CH}}$ and general-base catalysis is observed (Figure 3a). When phosphate buffer is employed, $K_{\text{CH}} > a_{\text{H}}$ and apparent general-acid catalysis is evident (Figure 4a).

In the presence of carbonate and phosphate buffers, a second considerably slower reaction is observed after enolization is complete. This reaction is catalyzed by the acids HCO_3^- and

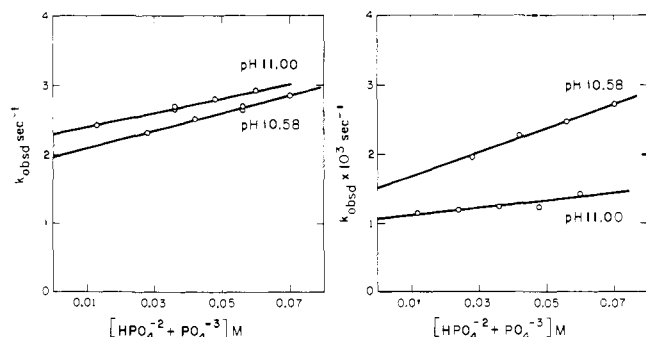


Figure 4. (a) Plots of the observed first-order rate constants for the initial reaction of diethyl oxaloacetate in the presence of phosphate ($\text{HPO}_4^{2-}/\text{PO}_4^{3-}$) buffer vs. the total concentration of phosphate buffer at three pH values. (b) Plots of the observed first-order rate constants for the second reaction evidenced by diethyl oxaloacetate in the presence of phosphate buffer.

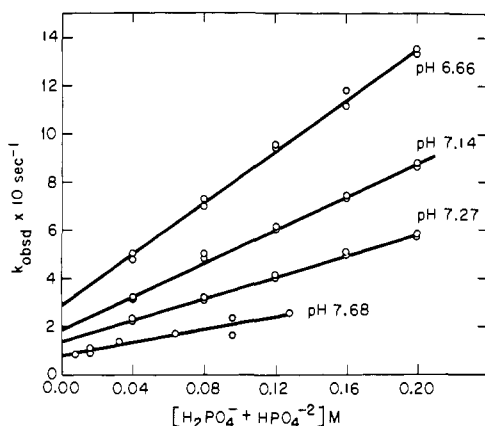


Figure 5. Plots of the observed first-order rate constants for the reaction of diethyl oxaloacetate in the presence of phosphate ($\text{H}_2\text{PO}_4^-/\text{HPO}_4^{2-}$) buffer at four hydrogen-ion concentrations.

HPO_4^{2-} (Figures 3b and 4b). The intercepts of these buffer dilution plots are indicated by the squares on line b of Figure 2 between pH 9.2 and 11.2. The location of these intercepts suggests that this general-acid-catalyzed reaction pertains to the dehydration-hydration equilibrium of eq 12.

At neutral pH values in the presence of weakly basic buffers such as phosphate ($\text{H}_2\text{PO}_4^-/\text{HPO}_4^{2-}$, $\text{p}K_a$ 6.62) and imidazole ($\text{p}K_a$ 7.14), diethyl oxaloacetate evidences only one reaction. The buffer dilution plots, as shown in Figure 5 for phosphate buffer, demonstrate the rate to be dependent on the concentration of the acid component of the buffer. Like results were obtained for imidazole buffer solutions where the catalytic entity is the protonated imidazolium ion. The intercepts of the phosphate and imidazole buffer dilution plots (indicated by squares on line b of Figure 2 in the pH range 6.0–7.2) fall on the same pH–rate profile as the intercepts of the second of the two consecutive rates observed in the presence of the more basic buffer systems. In addition, the second-order general-acid catalytic rate constants for phosphate and imidazole fall on the Brønsted plot established for dehydration (Figure 6). It is, therefore, reasonable to assign the acid-catalyzed reaction evidenced in the presence of these buffers to the hydration–dehydration reaction of eq 12. Below pH 8, dehydration in the absence of buffer is faster than keto–enol interconversion (Figure 2). However, it is the slower of the two consecutive reactions that is measured in the presence of buffer species and that is ascribed to dehydration. This requires that the rate constant for dehydration be less sensitive than the rate constant for keto–enol interconversion to a change in concentration of buffer species (Figure 7a). The buffer dilution plots of Figure

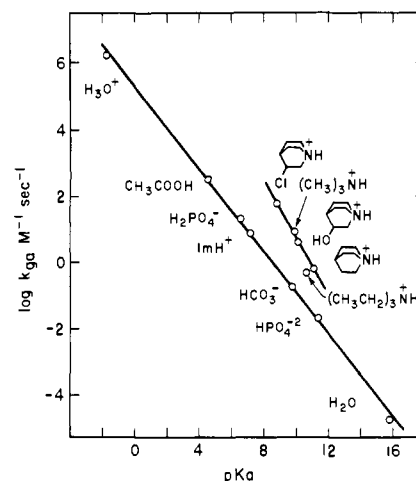


Figure 6. Logarithmic plots of the second-order general-acid catalytic rate constants vs. the $\text{p}K_a$ of the general acid.

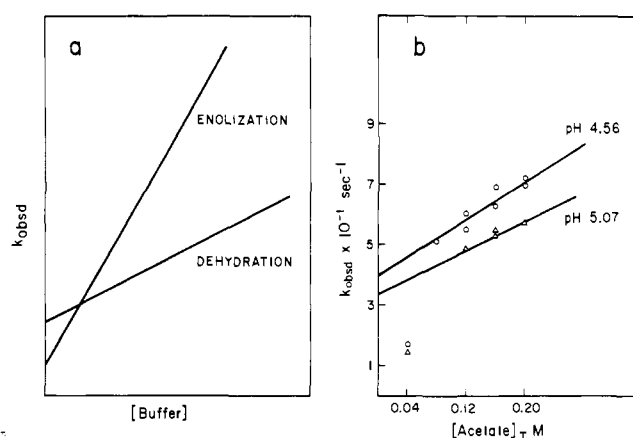


Figure 7. (a) Relative dependence of enolization and dehydration rate constants on buffer concentration. (b) Plots of the observed first-order rate constants for the reaction of diethyl oxaloacetate in the presence of acetate buffer vs. the total concentration of acetate buffer at two pH values.

7b were obtained for the reaction of diethyl oxaloacetate in the presence of acetic acid buffer systems. As in the case of the phosphate and imidazole buffer dilution plots, the intercepts of the acetic acid buffer dilution plots fall on the pH–rate profile for dehydration. The large negative deviations obtained for the observed rate constants at the lowest buffer concentration suggest crossover of the buffer dilution plots for general-acid-catalyzed dehydration and keto–enol interconversion as diagrammed in Figure 7a. Reaction rates in the presence of phosphate, imidazole, and acetate buffers were determined with a stopped-flow spectrophotometer. Only the rate constant (circles and triangles on profile a of Figure 2) for keto–enol interconversion is observed under acidic conditions when employing the pH–stated Cary 15 spectrophotometer. Dehydration presumably occurs too rapidly for its rate to be detected with this instrument.

The logarithms of the second-order rate constants for general-acid catalysis of the dehydration reaction of eq 12 are plotted in Figure 6 vs. the $\text{p}K_a$ of the general-acid catalyst. A good linear correlation is obtained over $\sim 18 \text{ p}K_a$ units, resulting in a $-\alpha$ value of 0.62. The kinetically equivalent mechanism of preequilibrium protonation followed by general-base-catalyzed expulsion of water can be ruled out, since the second-order rate constants would be diffusion controlled ($\sim 9 \times 10^9 \text{ M}^{-1} \text{ s}^{-1}$), thus requiring a Brønsted α value close to zero.¹² Reversible hydration reactions are generally associated with both general-acid and general-base catalytic terms.⁹ That only general-acid catalysis is detected in the de-

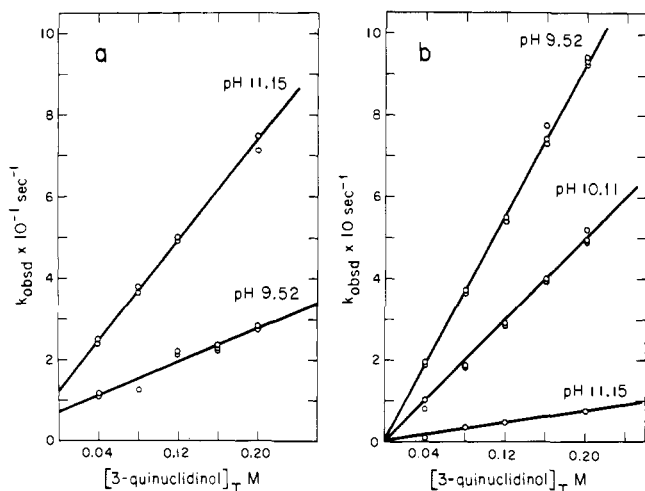
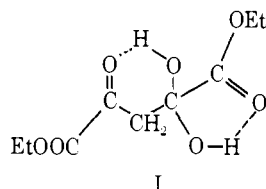


Figure 8. (a) Plots of the observed first-order rate constants for the reaction of diethyl oxaloacetate with 3-quinuclidinol vs. the total concentration of 3-quinuclidinol at two hydrogen ion concentrations. (b) Plots of the observed first-order rate constants for the second reaction evidenced by diethyl oxaloacetate in the presence of 3-quinuclidinol.

hydration of diethyl oxaloacetate suggests that intramolecular hydrogen bonding of the gem diol to the ester groups (I) de-



creases the rate of base-catalyzed dehydration by increasing the pK_a of the hydroxyl groups. This would also account for the small, when compared to that for other hydration-dehydration reactions, second-order rate constant for catalysis by hydroxide ion.^{9b,d,f}

Reaction of Diethyl Oxaloacetate with Tertiary Amines. The reaction of diethyl oxaloacetate was investigated in the presence of five tertiary amines of $pK_a > 8$. All of the tertiary amines gave buffer dilution plots which show the free base form of the amine to be the reactive species. Representative amine buffer dilution plots are shown in Figure 8a for reaction of diethyl oxaloacetate with 3-quinuclidinol (pK_a 10.11). Because of the degree of steepness of the k_{obsd} vs. $[N]_T$ plots (where $[N]_T = \text{total amine buffer} = [N] + [NH]$), the intercepts at zero amine concentration of several of these plots could not be obtained. Those intercepts that could be determined are plotted in Figure 2; the dashed line drawn through these points corresponds to a k_{obsd} value of 12.3 s^{-1} . Since the intercept values are as much as 25-fold greater than the rate of reaction of diethyl oxaloacetate with lyate species at the same pH (line a of Figure 2), it is apparent that the amine buffer dilution plots of Figure 8a do not represent the reaction of amine with diethyl oxaloacetate according to the general-base-catalyzed mechanism of eq 14. These observations are identical to those evidenced in the reaction of oxaloacetate with tertiary amines (see Figure 2 of the preceding paper)¹ which were explained by the nucleophilic addition-elimination reaction of eq 1. Thus, it would appear that diethyl oxaloacetate, like oxaloacetic acid, forms a zwitterionic carbinolamine intermediate (C^\pm) with tertiary amines (eq 16). Protonation of C^\pm prevents its collapse back to starting materials. Enolization then occurs as a result of a second molecule of tertiary amine abstracting a proton from the α -carbon of C^+ causing the elimination of neutral amine. Water and hydroxide ion can also act as catalysts in the elimination reaction. The mechanism of eq 16 proposes that

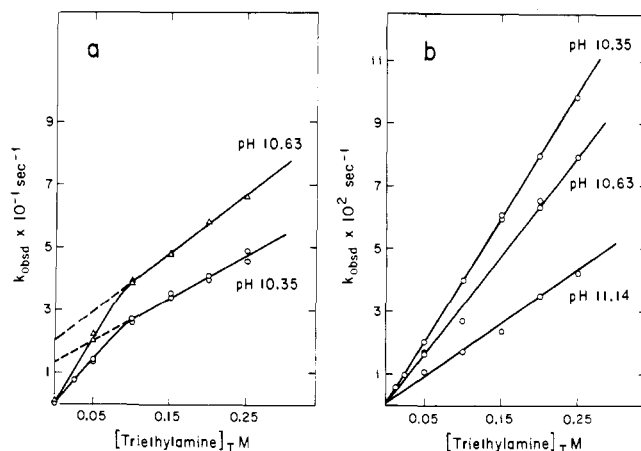
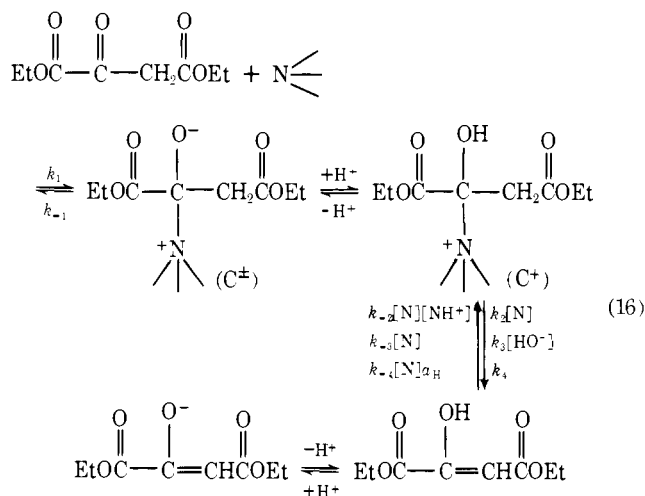


Figure 9. (a) Plots of the observed first-order rate constants for the reaction of diethyl oxaloacetate and triethylamine vs. the total concentration of triethylamine at two hydrogen-ion concentrations. Intercepts at $[N]_T = 0$ for the solid-line buffer dilution plots were obtained from the pH-rate profile a of Figure 2. Intercepts obtained by extrapolating rates determined at high $[N]_T$ to $[N]_T = 0$ (dashed lines) are plotted on the dashed line of Figure 2. (b) Plots of the observed first-order rate constants for the second reaction evidenced by diethyl oxaloacetate in the presence of triethylamine.



the amine-catalyzed elimination reaction occurs predominately through the protonated intermediate (C^+). In order that the first-order dependence on $[N]$ be observed (Figures 8a and 9a), elimination through the zwitterionic carbinolamine (C^\pm) would require the second-order rate constant for elimination to be substantially larger than the rate of collapse of C^\pm back to starting materials, not a likely situation.

Assumption of a steady-state concentration of C^\pm and C^+ as established for oxaloacetic acid results in the rate expression of eq 17 where K_{C^+} , K_E , and K_A are the acid-dissociation

$$k_{\text{obsd}} = k_f + k_r = \frac{k_1 k_2 a_H [N]^2 + k_1 (k_3 K_w + k_4 a_H) [N] + \left(\frac{a_H}{K_E + a_H} \right) \times k_{-1} K_{C^+} (k_{-2} a_H [N] / K_A + k_{-3} + k_{-4} a_H) [N]}{k_2 a_H [N] + k_{-1} K_{C^+} + k_3 K_w + k_4 a_H} \quad (17)$$

$$k_{\text{obsd}} = k_f + k_r = \frac{a_H (k_1 k_2 + \left(\frac{a_H}{K_E + a_H} \right) k_{-1} k_{-2} K_{C^+} / K_A) [N]^2 + a_H (k_1 k_4 + \left(\frac{a_H}{K_E + a_H} \right) k_{-1} k_{-3} K_{C^+} / a_H + k_1 k_3 K_w / a_H) [N]}{k_2 a_H [N] + k_{-1} K_{C^+} + k_3 K_w + k_4 a_H} \quad (18)$$

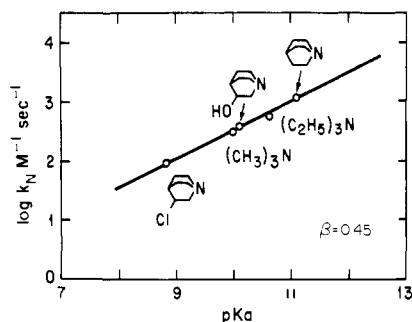


Figure 10. Brønsted plot for the reaction of tertiary amines with diethyl oxaloacetate.

constants of C^+ , enol, and tertiary amine, respectively. Since $k_{-3} > k_{-4}a_H$, eq 17 rearranges to eq 18. That the reaction of amine with diethyl oxaloacetate is not linear in amine at all amine concentrations is evidenced by the buffer dilution plots for reaction with triethylamine (Figure 9a). At high amine concentration the reaction rate is linearly dependent on amine concentration, and the intercepts given by extrapolation of the linear portion of the buffer dilution plots (dashed lines) are plotted on the dashed line of Figure 2. The rate constants at zero amine concentration to which the solid lines of Figure 9a are drawn were taken from the pH-rate profile a of Figure 2 at the appropriate hydrogen-ion concentrations.

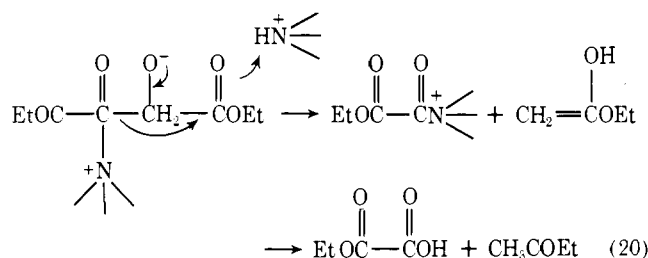
At amine concentrations which give rise to a linear dependence of observed rate constant on amine concentration (eq 18 with $k_2a_H[N] > k_{-1}K_{C^+} + k_3K_w + k_4a_H$), the observed rate constants can be expressed as in eq 19.

$$k_{\text{obsd}} = k_f + k_r = \left(k_1 + \frac{a_H}{K_E + a_H} \frac{k_{-1}k_{-2}K_{C^+}}{k_2K_A} \right) [N] + \frac{k_1k_4}{k_2} + \frac{k_1k_3K_w}{k_2a_H} + \frac{a_H}{K_E + a_H} \left(\frac{k_{-1}k_{-3}K_{C^+}}{k_2a_H} \right) \quad (19)$$

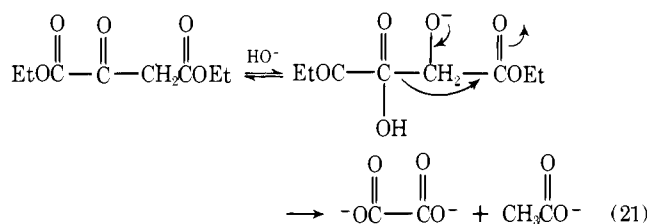
Equation 19 differs from the corresponding equation for the tertiary amine catalyzed enolization of oxaloacetic acid in that $K_E > a_H$ for the diester, while $K_E < a_H$ for the diacid. None of the tertiary amines employed as catalysts of keto-enol interconversion of diethyl oxaloacetate evidence the ammonium ion dependent term of eq 19. The second-order amine free base rate constants (k_N) obtained from buffer dilution plots such as those shown in Figures 8a and 9a thus pertain to the k_1 values of eq 19. The logarithms of these second-order rate constants are plotted in Figure 10 vs. the pK_a of the particular tertiary amine. The slope of the plot, β , is 0.45. This can be compared to the β value of 0.77 obtained from the Brønsted plot of the second-order rate constants for reaction of tertiary amines with oxaloacetic acid.¹ In the case of the diacid, however, it is not apparent whether the amine second-order rate constants are composite terms [$k_1 + (k_{-1}k_{-2}K_{C^+}/k_2K_A)$] or whether they too pertain simply to nucleophilic attack on ketone (k_1). Only the spontaneous term of eq 19 is evidenced by the intercepts of plots of k_{obsd} vs. $[N]_T$; the hydroxide ion dependent term is not observed (dashed line of Figure 2).

After the reaction of eq 16 is complete, a second slower reaction is observed in the presence of tertiary amines. The buffer dilution plots for this reaction are given in Figures 8b and 9b for reaction with 3-quinuclidinol and triethylamine. The pH dependence of the slopes of the plots indicates that protonated amine is the kinetically important species. The logarithms of the second-order general-acid catalytic rate constants are plotted in Figure 7 vs. the amine pK_a . The Brønsted $-\alpha$ value is 0.89. The magnitude of these second-order rate constants requires the amines to be acting as general-acid catalysts, since

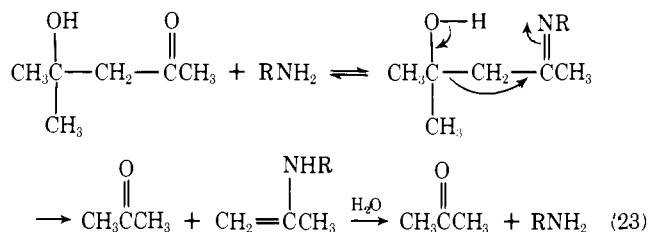
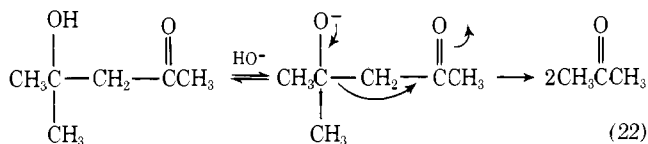
any mechanism involving amine nucleophilic catalysis upon a protonated substrate species would result in the second-order rate constants being beyond diffusion controlled unless the amine were acting on a species with a $pK_a > 1$. The observation of general-acid catalysis with amines of $pK_a > 8$ requires that these species have a $pK_a < 8$. Neither the ketone, enol, hydrate, nor carbinolamine has a pK_a in this region. The more than 100-fold separation in the two Brønsted plots of Figure 7 and the substantially different β values indicate that the tertiary amines are not catalyzing the same reaction catalyzed by the other general acids, i.e., the reversible dehydration reaction of eq 12. The amines, therefore, must be acting as general-acid catalysts on a species that exists only in the presence of tertiary amines such as the carbinolamine intermediate. A possible candidate for the reaction under consideration is a rate-limiting general-acid-catalyzed cleavage of the carbinolamine intermediate to ethyl oxalate and ethyl acetate after the enolization equilibrium of eq 16 has reached completion (eq 20). Diethyl



oxaloacetate is known to undergo a cleavage reaction under basic conditions (eq 21).¹³ This is but one of a wide variety of



reactions involving hydrolytic cleavage of a carbon-carbon bond, including hydrolysis of acetylacetone,¹⁴ chloral hydrate,¹⁵ 2-nitroacetophenone,¹⁶ diethyl acetylmalonate, and diethyl acetylmalonate.¹⁷ These reactions all require basic catalysis, since the neutral hydrate does not possess sufficient driving force to cause expulsion of the carbanion. Base catalysis, however, is unnecessary if the cleavage reaction occurs through the carbinolamine zwitterion. General-acid catalysis by amine serves to increase the leaving tendency of the departing carbanion. Diacetone alcohol undergoes a hydroxide ion catalyzed dealdolization reaction (eq 22).¹⁸ This reaction



has been found to be catalyzed by primary amines (and to a lesser extent by secondary amines), and the proposed mechanism involves formation of a Schiff base intermediate (eq 23).¹⁹

Acknowledgement. The authors are extremely grateful to Susan Crase Wilson for her superior technical assistance. This work was supported by a grant from the National Institutes of Health.

References and Notes

- (1) P. Y. Bruice and T. C. Bruice, *J. Am. Chem. Soc.*, preceding paper in this issue.
- (2) B. E. Banks, *J. Chem. Soc.*, 63 (1962).
- (3) E. S. Hand and W. P. Jencks, *J. Am. Chem. Soc.*, **97**, 6221 (1975).
- (4) A. F. Hegarty and W. P. Jencks, *J. Am. Chem. Soc.*, **97**, 7188 (1975).
- (5) J. R. Maley and T. C. Bruice, *Anal. Biochem.*, **34**, 275 (1970).
- (6) G. Schwarzenbach and E. Felder, *Helv. Chim. Acta*, **27**, 1701 (1945).
- (7) R. P. Bell, "The Proton in Chemistry", Cornell University Press, Ithaca, New York, 1973, p 41.
- (8) S. S. Tate, A. K. Grzybowski, and S. P. Datta, *J. Chem. Soc.*, 1372 (1964).
- (9) (a) R. P. Bell, "Advances in Physical Organic Chemistry", Vol. IV, V. Gold, Ed., Academic Press, New York, N.Y., 1966, p 1; (b) R. P. Bell, M. H. Rand, and K. M. A. Wynne-Jones, *Trans. Faraday Soc.*, **52**, 1093 (1956); (c) L. C. Gruen and P. T. McGuire, *J. Chem. Soc.*, 5224 (1963); (d) R. P. Bell and P. G. Evans, *Proc. R. Soc. London, Ser. A*, **291**, 297 (1966); (e) J. P. Guthrie, *J. Am. Chem. Soc.*, **94**, 7020 (1972); (f) Y. Pocker and D. G. Dickerson, *J. Phys. Chem.*, **73**, 4005 (1969); (g) Y. Pocker, J. Meany, and C. Zadorojny, *J. Phys. Chem.*, **75**, 792 (1971).
- (10) F. C. Kokesh, *J. Org. Chem.*, **41**, 3593 (1976).
- (11) M. Charton, *J. Org. Chem.*, **29**, 1222 (1964).
- (12) M. Eigen, *Angew. Chem., Int. Ed. Engl.*, **3**, 1 (1964).
- (13) "Chemistry of Carbon Compounds", Vol. 1B, E. H. Rodd, Ed., Elsevier, Amsterdam, 1952, p 1132.
- (14) R. G. Pearson and E. A. Mayerle, *J. Am. Chem. Soc.*, **73**, 926 (1951).
- (15) (a) C. Gustafsson and M. Johanson, *Acta Chem. Scand.*, **2**, 42 (1948); (b) E. Pfeil, H. Stache, and F. Lömker, *Ann. Chem.*, **623**, 74 (1959).
- (16) R. G. Pearson, D. H. Anderson, and L. L. Alt, *J. Am. Chem. Soc.*, **77**, 527 (1955).
- (17) G. E. Lienhard and W. P. Jencks, *J. Am. Chem. Soc.*, **87**, 3855 (1965).
- (18) C. C. French, *J. Am. Chem. Soc.*, **51**, 3215 (1959).
- (19) (a) M. L. Miller and M. J. Kilpatrick, *J. Am. Chem. Soc.*, **53**, 3217 (1931); (b) F. H. Westheimer and H. J. Cohen, *J. Am. Chem. Soc.*, **60**, 90 (1938); (c) M. L. Bender and R. Breslow, *Compr. Biochem.*, **2**, 150 (1962); (d) R. M. Pollack and S. Ritterstein, *J. Am. Chem. Soc.*, **94**, 5064 (1972).

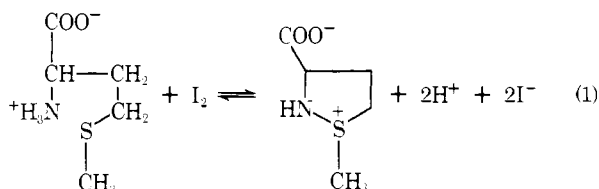
Reduction of Dehydromethionine by Thiols. Kinetics and Mechanism^{1a}

David O. Lambeth^{1b}

Contribution from the Department of Biochemistry, School of Medicine, The University of North Dakota, Grand Forks, North Dakota 58202. Received January 16, 1978.

Abstract: Dehydromethionine (*S*-methylisothiazolidine-3-carboxylate) reacts with dithiothreitol, 5-thio-2-nitrobenzoic acid, and 2-thio-5-nitropyridine to form methionine and the corresponding disulfides. The reaction is second order overall, being first order with respect to each reactant. The rate-limiting step is associated with the initial attack of thiol on the sulfur of dehydromethionine—completion of disulfide formation by the attack of the second thiol on the thiol-dehydromethionine addition intermediate occurs rapidly. The slopes of the pH-log rate profiles show breaks corresponding to the pK's of the thiols used and thus implicate the thiolate anion as the attacking nucleophile. The reactions are strongly catalyzed by the acid components of phosphate, imidazole, acetate, and formate buffers, the increase in rate being as much as 100- to 1000-fold with 0.1 M phosphate buffers. The rate-determining step is proposed to be a general-acid-catalyzed S_N2 displacement reaction in which thiolate anion attacks the sulfur of dehydromethionine concerted with protonation of the nitrogen of dehydromethionine resulting in its expulsion as a neutral amine.

Dehydromethionine (*S*-methylisothiazolidine-3-carboxylate) is a cyclic sulfonium derivative of methionine first prepared by Lavine.² The compound may be variously considered as an azasulfonium salt or a cyclic, N-protonated sulfilimine or sulfimide. Dehydromethionine is formed as the immediate product of the iodinic oxidation of methionine in neutral solution (eq 1), and the reaction is rapidly and quantitatively



reversed upon acidification of the solution. The structure of dehydromethionine has been verified by the recent X-ray diffraction study of Glass and Duchek.³

Iodinic oxidation of thioethers in aqueous solution normally results in the formation of sulfoxides. However, with methionine, formation of dehydromethionine rather than methionine sulfoxide occurs due to an approximation effect⁴ resulting in a very favorable intramolecular attack of the amino group on

an iodo-sulfonium intermediate. Dehydromethionine is stable indefinitely when stored over desiccant and its half-life in neutral aqueous solutions in the absence of buffer species is estimated to be 600 days.⁵ Hydrolysis of dehydromethionine to form the sulfoxide is strongly catalyzed by a number of buffers, and the pH-log rate profile for the reaction shows a minimum near 7 with slopes of +1 and -1 above and below pH 7, respectively.⁵

Although dehydromethionine has been known for over 30 years, the literature on this substance is limited to the references cited above. In fact, apart from dehydromethionine, isothiazolidines as unicyclic structures appear to be unknown entities.

Lavine reported without supporting evidence that dehydromethionine is reduced by thiols.^{2c} Since such a reaction would set one boundary condition for the existence of dehydromethionine-like (azasulfonium) compounds in biological systems, we undertook the study reported here to determine the characteristics of the reaction. The presence of the azasulfonium linkage in biochemical systems seems plausible in view of the ubiquity of amine and thioether functional groups and the ease with which the linkage can be formed.

We have found the reduction of dehydromethionine to be